

Sensitivity of ice-cemented Antarctic soils to greenhouse-induced thawing: Are terrestrial archives at risk?

Kate M. Swanger*, David R. Marchant

Department of Earth Sciences, 685 Commonwealth Avenue, Boston University, Boston, MA 02215, USA

Received 9 August 2006; received in revised form 6 April 2007; accepted 27 April 2007

Available online 8 May 2007

Editor: H. Elderfield

Abstract

We modeled the sensitivity of six ice-cemented slope deposits from the western McMurdo Dry Valleys, Antarctica to failure by shallow, thaw-induced planar sliding. The deposits examined have purportedly remained physically stable, without morphologic evidence for downslope movement, for millions of years. Could they fail in the near future from greenhouse-induced warming? To address this question, we first prescribed various increases in mean summertime soil surface temperature (MSSST) and modeled numerically the resultant changes in soil thaw depths using a one-dimensional heat diffusion equation (including the effects of latent heat of fusion). Second, we calculated the minimum thaw depths required to facilitate failure by shallow planar sliding for each deposit; for all numerical simulations, we maintained present soil-moisture conditions and used a Mohr–Coulomb-based equation of safety factor. Third, we calculated the rate of subsurface meltwater flow assuming Darcy's Law. Our results show that although most deposits contain sufficient subsurface ice to induce sliding upon thawing, lateral rates of water flow of as much as ~40 m/day for some colluvial deposits prohibit the build-up of requisite pore pressures for failure. On the other hand, silty deposits, that contain gravimetric water $\geq 15\%$, occur on slopes $>20^\circ$, and possess low hydraulic conductivities (~30–60 cm/day), common in the Dry Valleys region, could fail if MSSST, and by inference mean summertime atmospheric temperatures, increase by 4 to 9 °C. This temperature increase is similar to that predicted to occur from greenhouse-induced warming in Antarctica over the next century.

© 2007 Elsevier B.V. All rights reserved.

Keywords: planar sliding; permafrost; McMurdo Dry Valleys; thermal modeling; slope stability; climate change

1. Introduction

The western region of the McMurdo Dry Valleys (MDV) is one of the coldest and driest places on Earth (Fig. 1). The region has long been considered a frozen and nearly paralyzed landscape. Rates of bedrock

erosion, as deduced from cosmogenic exposure-age studies, are as low as 5–10 cm Ma⁻¹ (Brook et al., 1993; Ivy-Ochs et al., 1995; Summerfield et al., 1999; Schaefer et al., 1999, 2000; Margerison et al., 2005), and the preservation of in situ, near-surface ashfall as much as 10–15 Ma (⁴⁰Ar/³⁹Ar dating) implies that in places there has been limited bedrock erosion and colluviation for millions of years (Marchant et al., 1993a, 1996) (Fig. 2). Together, these data suggest that most of the unconsolidated landforms and bedrock features of the western Dry Valleys region are relict

* Corresponding author. Tel.: +1 617 353 6967; fax: +1 617 353 3290.

E-mail address: kswanger@bu.edu (K.M. Swanger).

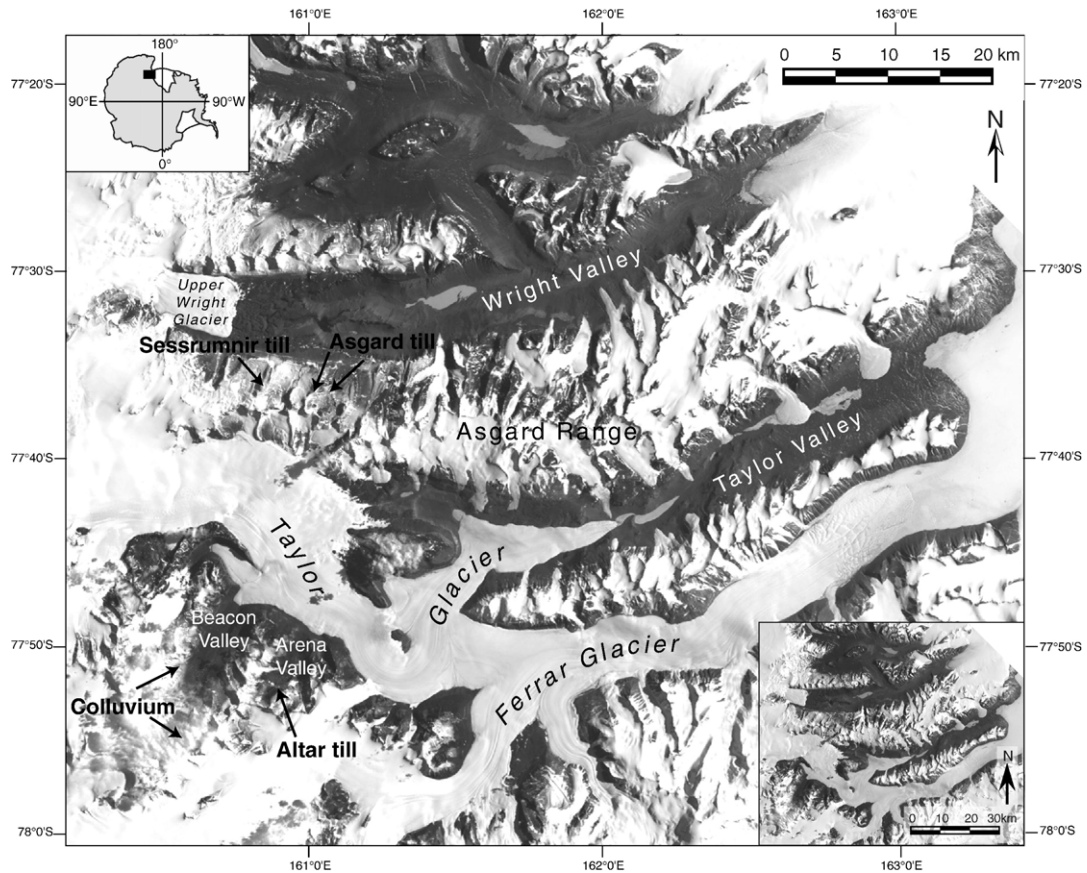


Fig. 1. Satellite image of the McMurdo Dry Valleys. Upper left inset: location map of the Dry Valleys. Lower right inset: map of Dry Valleys showing the geographic distribution of the coastal thaw zone (black), inland mixed zone (dark grey) and stable upland zone (light grey).

(Summerfield et al., 1999; Marchant et al., 1996; Sugden et al., 1995). Given the long-term geomorphic stability of the region, and by inference the long-term climate stability (Marchant and Denton, 1996), a reasonable question to ask is how might an increase in atmospheric temperature influence the morphology and preservation of unconsolidated landforms?

The geomorphic impact of warming is already noted in Antarctica between 60° and 70°S, and is manifested as a thinning of some ice shelves (Scambos et al., 2003). In the Arctic, there is considerable geomorphic evidence for greenhouse-induced thawing of permafrost; such thawing deepens seasonal active layers and increases the rates of shallow slope failures (Davies et al., 2001; Harris et al., 2001). Will future warming in the western MDV, a general prediction of most climate models (Intergovernmental Panel on Climate Change (IPCC), 2001, see also Doran et al., 2002a), lead to thaw instability of ice-cemented slope deposits? Or, are these deposits relatively insensitive to increases in atmospheric temperature? To address these questions

we modeled the potential for thaw-induced slope failure for typical ice-cemented deposits found throughout the western MDV (78°S) (Fig. 1). We assume that the driving force for planar slides arises from elevated pore pressures generated by the in situ melting of interstitial ice [e.g., McRoberts and Morgenstern, 1974].

2. Setting

2.1. Landscape stability and microclimate zonation

The sensitivity of unconsolidated deposits to thaw-induced planar sliding is, to a large extent, dictated by local environmental conditions. The MDV are commonly subdivided into a series of discrete microclimate zones (Fig. 1), each displaying a different propensity for modern slides and for future sliding with soil warming. The three microclimate zones depicted in Fig. 1 (right inset) are defined based on summertime atmospheric temperatures and soil-moisture conditions (Table 1).

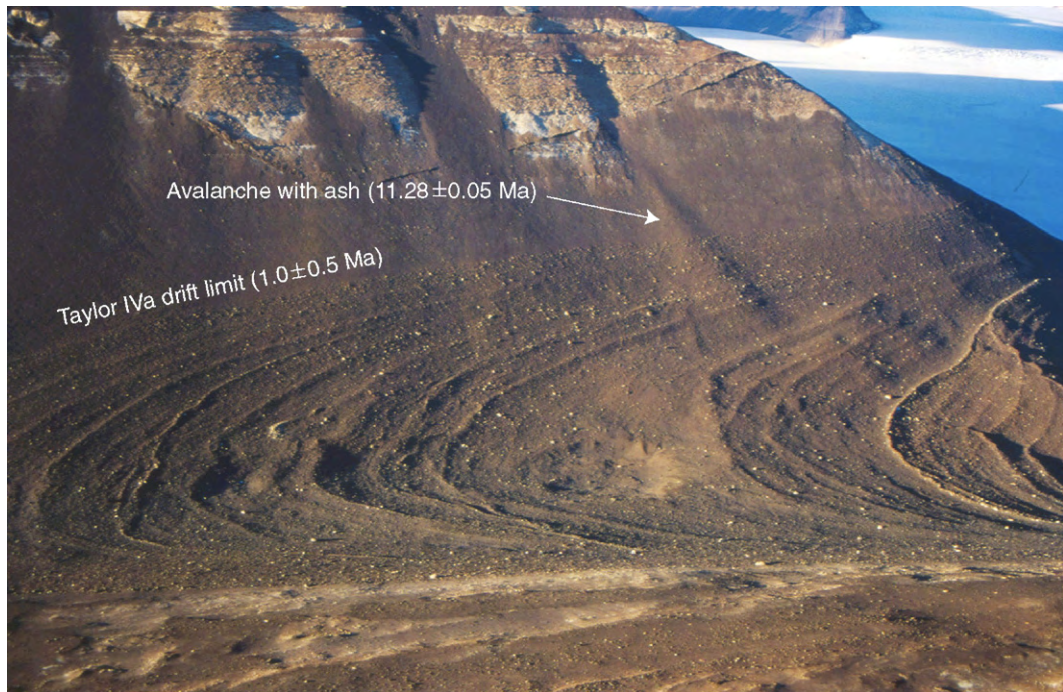


Fig. 2. Oblique aerial photograph of lower Arena Valley, Quartermain Mountains, looking to the northwest. On the valley wall and bottom are a series of arcuate moraines deposited from a cold-based lobe(s) of Taylor Glacier. The minimum age for the uppermost moraine, based on ^{10}Be cosmogenic-exposure age analyses is 1.0 ± 0.5 Ma (Brook et al., 1993; Marchant et al., 1994). This moraine, along with several additional lower-elevation moraines, cross a well-preserved avalanche deposit (arrowed) that, in turn, rests on dolerite colluvium 28° to 32° . Sandstone bedrock crops out near the top of the photograph. The unconsolidated avalanche deposit contains $\sim 30\%$ volcanic ash in the matrix (< 2 mm) fraction. Volcanic crystals (sanidine) from this deposit date to 11.28 ± 0.05 Ma ($^{40}\text{Ar}/^{39}\text{Ar}$ dating (Marchant et al., 1993a)), and provide an age for the avalanche cone. Neither the ash avalanche deposit nor the moraines that cross the slope show morphologic evidence for post-depositional modification and/or erosion from downslope movement. The deposits emphasize the long-term geomorphic stability of the stable upland zone, McMurdo Dry Valleys (see also Marchant and Head (Marchant and Head, in press)).

They include a coastal thaw zone, in which soils exhibit a dynamic active layer, a stable upland zone, in which moisture content and soil temperatures are too low to generate typical active layer processes, and an intermediate mixed zone, which represents a transition

Table 1
Climate data: yearly averages (12/31/00 to 12/31/02) from the stable upland and coastal thaw zones

	Upland ^a	Coastal ^b
Mean summer air T ($^\circ\text{C}$) ^c	-10	-5
Days max air $T > 0$ $^\circ\text{C}$	7	46
Max air T ($^\circ\text{C}$)	3	12
Mean summer soil T at 0 cm depth ($^\circ\text{C}$)	-5	2
Mean summer soil T at 10 cm depth ($^\circ\text{C}$)	-6	1
Days max soil T at 0 cm depth is > 0 $^\circ\text{C}$	80	106
Days max soil T at 10 cm depth is > 0 $^\circ\text{C}$	15	75

^a Beacon Valley, 1176 m above sea level, 74 km from coast.

^b Explorers Cove, 26 m above sea level, 4 km from the coast.

^c Summer months: December, January, February. Data from Long-term Ecological Research: huey.Colorado.edu/LTER/meteorodata.html.

between these two end members (Marchant and Denton, 1996; Marchant and Head, in press) (Table 1). Ice-cemented deposits in the coastal thaw zone show evidence for subsurface melt, including thermokarst, solifluction, and shallow planar slides. Such melting does not occur in the upland zone (Denton and Marchant, 2000), where many upland slopes appear to be stable on million-year time-scales (Figs. 1 and 2) (Marchant et al., 1994). If the climate conditions that characterize the coastal thaw zone should advance inland (Table 1), will slope deposits of the stable upland zone similarly fail by shallow planar sliding [e.g., Marchant and Denton, 1996]?

2.2. Ice-cement in Dry Valley soils

Ice-cement is ubiquitous in most soils of the MDV. The depth to the ice-cement table can be variable within a single deposit, but it commonly lies ~ 10 – 50 cm deep. In most cases the maximum depth (base)

of ice-cemented soil is unknown (owing to the difficulty of physically excavating ice-cemented soils), but it most probably exceeds 2 m (based on direct examination of shallow cores from throughout the MDV) (Stuiver et al., 1981; Pringle et al., 2006). The presence of this subsurface ice is perplexing due to the extremely cold and arid conditions of the region. Some theoretical models characterizing sublimation processes in soils of the MDV suggest that subsurface glacier ice and/or ice cement is unstable and should sublime after a few thousand years (Hindmarsh et al., 1998; McKay et al., 1998). However, recent numerical models incorporating high-resolution soil temperature data have shown that sublimation of buried ice may be much slower than originally thought, due, in part, to the fact that vapor moves both downward and upward through deposits. The downward movement of vapor retards ice sublimation and can potentially add ice at depth (Kowalewski et al., 2006; Marchant et al., 2002). On average, soils in the coastal thaw zone contain more moisture and have shallower ice-cement tables than do soils of the inland mixed and stable upland zones (Campbell et al., 1997a; Campbell and Claridge, 2006). This is due, in part, to local recharge from the melting of glaciers and snow banks in the coastal zone, a process that is largely absent from the stable upland zone (Marchant and Denton, 1996; see also Discussion).

3. Methods

3.1. Sample collection and laboratory analyses

We excavated a series of soil pits (each $\sim 0.75 \text{ m}^3$) in coarse-grained dolerite colluvium and in fine-grained, silty drifts throughout the stable upland zone (Fig. 1). At each excavation, we collected a suite of sediment samples at 5-cm depth increments; each sample included a matrix fraction ($<16 \text{ mm}$) and a gravel fraction (16 mm to 64 mm). The matrix fraction ($\sim 2 \text{ kg}$) was sieved at half-phi intervals at Boston University and plotted as frequency curves (Fig. 3), and the coarse-gravel fraction ($\sim 10 \text{ kg}$) was analyzed for grain shape, lithology, and surface texture. Visual inspection of the ice-cemented portion of all deposits showed no obvious variation in ice content and no discrete ice lenses. The gravimetric water content (GWC, $\text{mass}_{\text{water}}/\text{mass}_{\text{dry soil}}$) was calculated by placing samples in a pre-weighed beaker, weighing to $\pm 0.005 \text{ g}$, drying for 12 h at 100°C , and then re-weighing with equal precision (Table 2). Replicate analyses showed consistent and uniform results to within 0.5%.

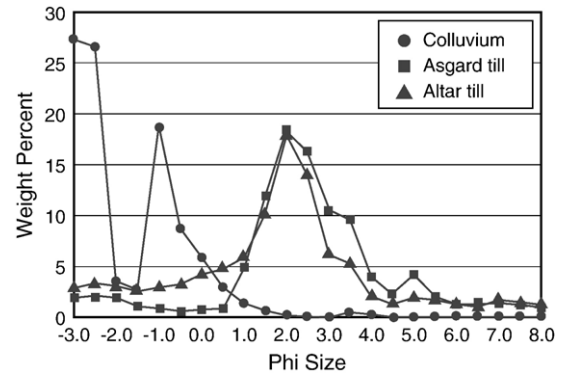


Fig. 3. Grain size distribution of the $<16\text{-mm}$ fraction for Altar till, Asgard till, and dolerite colluvium; the median grain size for dolerite colluvium is -2.5ϕ (fine gravel), whereas that for Altar till and Asgard till is $+2.0 \phi$ (medium sand).

3.2. Modern climate and soil conditions

We deployed a series of micro station data loggers (HOBO products, Onset Computer Corporation) to record solar radiance, atmospheric temperature, atmospheric relative humidity, soil temperature, and soil moisture at two sites. Readings were collected automatically at 15-min intervals from November 23 to December 9 in upper Beacon Valley and from November 18 to December 29 in central Beacon Valley (Fig. 4). For the purposes of this paper, measured conditions, similar at both sites (Fig. 4), are generally applicable to all our studied sites (see also Doran et al., 2002b).

4. Deposit characteristics

4.1. Coarse-grained deposits

4.1.1. Dolerite colluvium

All deposits of dolerite colluvium in our study area show a loose, surface cap of angular cobbles that rests on poorly stratified medium- to coarse-grained sands and medium- to fine-grained gravels. In most cases, the a -axes of surface and subsurface clasts are oriented parallel with the ground slope (generally ranging from 25° to 32°). The $<16\text{-mm}$ fraction (dry or ice-cemented) is typically comprised of 40–60% medium-to-fine gravel, 35–55% sand, and $<3\%$ silt and clay (mud) (Fig. 3). The depth to ice cement varies from ~ 10 to 15 cm (Table 2), and the GWC of the ice cement averages from 10% to 20% (Table 2). Soil moisture above the ice-cement table averages $<2\%$ GWC, a value consistent with earlier measurements of GWC in the stable upland zone (e.g., $<3\%$ (Campbell et al., 1997a;

Table 2
Summary of model parameters for the six sensitivity tests

Parameter	Dolerite colluvium (1)	Dolerite colluvium (2)	Asgard till (1)	Asgard till (2)	Sessrumnir till	Altar till
θ (slope angle)	32°	25°	15°	15°	20°	25°
ϕ' (effective angle of internal friction) ^a	35°	30°	25°	25°	28°	30°
z_{IC} (average depth to ice cement)	8 cm	12 cm	10 cm	10 cm	10 cm	10 cm
GWC of ice cement	12%	20%	15%	20%	15%	15%
VWC when ice thawed	20%	34%	28%	35%	28%	28%
γ_D (unit weight of dry soil)	1680 kg/m ³	1680 kg/m ³	1855 kg/m ³	1750 kg/m ³	1855 kg/m ³	1855 kg/m ³
γ_W (unit weight of water)	1000 kg/m ³	1000 kg/m ³	1000 kg/m ³	1000 kg/m ³	1000 kg/m ³	1000 kg/m ³
γ (unit weight of soil)	Varies with depth	Varies with depth	Varies with depth	Varies with depth	Varies with depth	Varies with depth
c' (effective cohesion) ^a	0.245 kN/m ²	0.245 kN/m ²	0.245 kN/m ²	0.245 kN/m ²	0.245 kN/m ²	0.245 kN/m ²
Specific gravity of sediments	2800 kg/m ³	2800 kg/m ³	2650 kg/m ³	2650 kg/m ³	2650 kg/m ³	2650 kg/m ³
p (porosity)	40%	40%	30%	35%	30%	30%
κ_D (dry diffusivity) ^b	3×10^{-7} m ² /s	3×10^{-7} m ² /s	3×10^{-7} m ² /s	3×10^{-7} m ² /s	3×10^{-7} m ² /s	3×10^{-7} m ² /s
κ_{IC} (ice-cemented diffusivity) ^b	1×10^{-6} m ² /s	1×10^{-6} m ² /s	1×10^{-6} m ² /s	1×10^{-6} m ² /s	1×10^{-6} m ² /s	1×10^{-6} m ² /s
κ_S (saturated diffusivity)	7×10^{-7} m ² /s	7×10^{-7} m ² /s	7×10^{-7} m ² /s	7×10^{-7} m ² /s	7×10^{-7} m ² /s	7×10^{-7} m ² /s
κ (average diffusivity used in modeling) ^c	7×10^{-7} m ² /s	7×10^{-7} m ² /s	7×10^{-7} m ² /s	7×10^{-7} m ² /s	7×10^{-7} m ² /s	7×10^{-7} m ² /s
c_i (total specific heat capacity of ice-cemented soil) ^d	956 J/kg °C	1060 J/kg °C	995 J/kg °C	1060 J/kg °C	995 J/kg °C	995 J/kg °C
c_i (specific heat capacity of ice)	2100 J/kg °C	2100 J/kg °C	2100 J/kg °C	2100 J/kg °C	2100 J/kg °C	2100 J/kg °C
c_w (specific heat capacity of water)	4184 J/kg °C	4184 J/kg °C	4184 J/kg °C	4184 J/kg °C	4184 J/kg °C	4184 J/kg °C
c_s (specific heat capacity of sediment)	800 J/kg °C	800 J/kg °C	800 J/kg °C	800 J/kg °C	800 J/kg °C	800 J/kg °C
k_H (hydraulic conductivity)	1×10^{-3} m/s	1×10^{-3} m/s	2×10^{-6} m/s	2×10^{-6} m/s	2×10^{-6} m/s	2×10^{-6} m/s
Ge (geometrical shape of pores) ^e	9×10^{-5}	9×10^{-5}	1×10^{-5}	1×10^{-5}	1×10^{-5}	1×10^{-5}
R_e (average pore size) ^f	3.2×10^{-6} m	3.2×10^{-6} m	1.2×10^{-6} m	1.2×10^{-6} m	1.0×10^{-6} m	1.0×10^{-6} m
Albedo ^g	0.07	0.07	0.07	0.07	0.07	0.07
Elevation range of deposit	~1800 m	~1500 m	1400–1600 m	1400–1600 m	1400–1600 m	~1500 m
Current maximum MSSST (mean summer soil surface temperature) ^h	-2 °C	-1 °C	-1 °C	-1 °C	-1 °C	-1 °C
Measured maximum penetration of 0 °C isotherm ^h	8 cm	12 cm	15 cm	15 cm	15 cm	15 cm

^a Angle of internal friction and cohesion were estimated from tests reported in Schellart et al. (2000). Angle of internal friction of silty deposits is generally less than that for sandy deposits. Cohesion is low in all deposits due to the lack of clay-sized particles.

^b We used the same dry, saturated and ice-cemented diffusivities for each deposit (after Campbell et al. (1997b) and our soil temperature measurements).

^c Determined by averaging the dry, saturated and ice-cemented diffusivities.

^d Determined from summing the heat capacities of ice and sediments multiplied by their respective weight percentages.

^e Determined using the hydraulic conductivities reported in Marchant et al. (2002) along with Darcy flow Eqs. (8) and (9).

^f Calculated with Eq. (10), using the grain size analyses reported in Fig. 3.

^g Albedo was held constant, although slight variations might vary due to the percentage of high-albedo sandstones at the ground surface.

^h Derived from our soil temperature measurements (Fig. 4).

Campbell and Claridge, 2006), see also (Kowalewski et al., 2006). The stratigraphic contact between the ice-cement table and overlying dry colluvium is sharp and planar. Near the boundary of perennial snowbanks and/or near the margin of large surface boulders, the contact may rise to within 3 cm of the ground surface.

4.2. Fine-grained deposits

Fine-grained deposits in the stable upland zone show a greater variation in the depth to the ice-cement table than do the coarse-grained colluvial deposits, varying from ~10-cm to >1 m. Just as for the case with the

colluvial deposits, the ice-cement table in fine-grained deposits also rises toward the margin of perennial snowbanks and/or large surface boulders. The GWC of ice cement in the fine-grained deposits appears visually uniform and, based on our field studies and published results from (Campbell et al., 1997a; Campbell and Claridge, 2006), is estimated at 10–20%.

4.2.1. Asgard till

Asgard till is a silt-rich deposit of mid-to-late Miocene age (14.8–13.6 Ma) that crops out in north-facing valleys of the western Asgard Range (Marchant et al., 1993b; Ackert, 1990). Granulometric analyses of

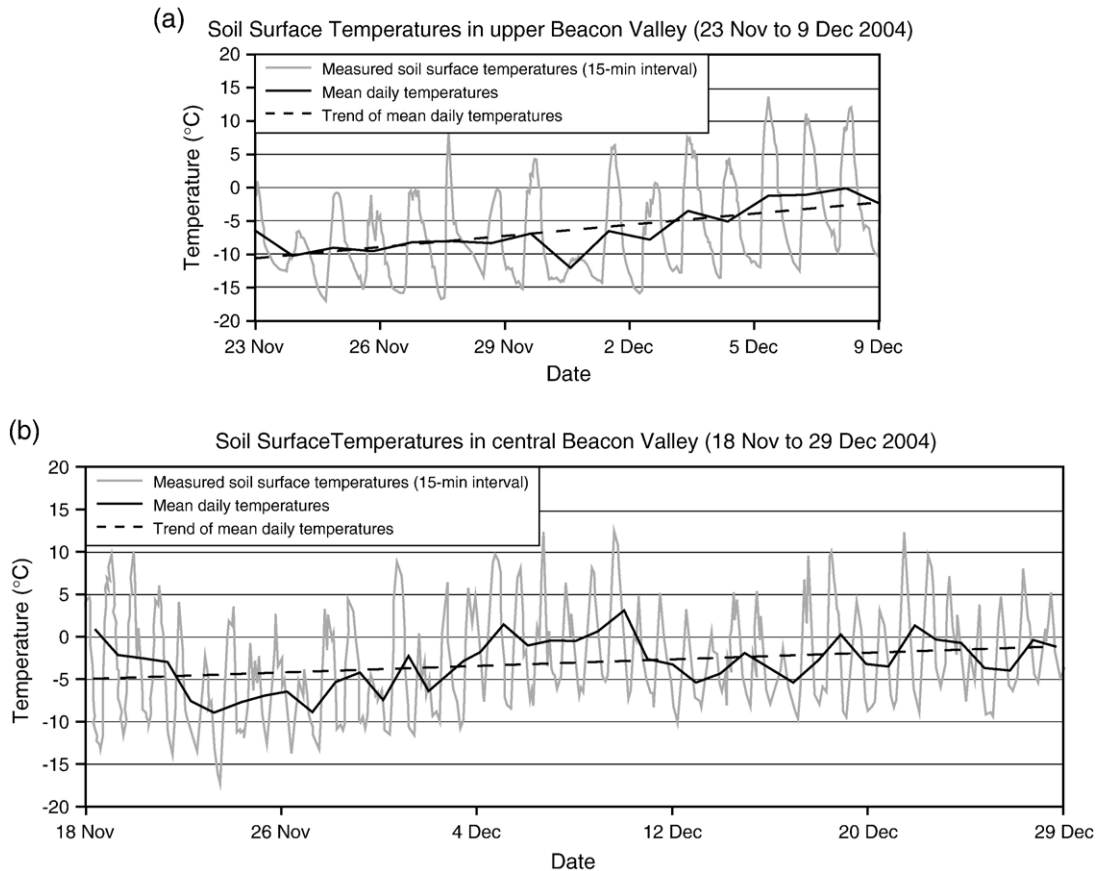


Fig. 4. Measured soil surface temperatures (recorded at 15-min intervals) used to model the current soil temperatures for the six sensitivity tests: (a) data from dolerite colluvium on a south-facing slope at 1800 m elevation in upper Beacon Valley; (b) data from the floor of central Beacon Valley (1350 m elevation). These data, along with season-long soil temperature data for central Beacon Valley (from Long-term Ecological Research (LTER): huey.Colorado.edu/LTER/meteordata.html; e.g., Fig. 5) were used to document soil temperature variability and to determine mean summertime soil surface temperatures (MSSST) for the stable upland region (for definition of MSSST, see Fig. 5).

35 samples of Asgard till show that it averages 10% gravel, 72% sand, and 18% mud (Fig. 3). The depth to ice cement varies from ~5 cm near perennial snowbanks to >1 m on some slopes and valley floors.

4.2.2. Altar till

Altar till is a highly oxidized, silt-rich deposit located in upper Arena Valley (Fig. 1). The till was likely deposited during mid-Miocene time, most probably >14.8 (Marchant et al., 1993a). On average, Altar till contains 27% gravel, 60% sand, and 13% mud (Fig. 3). The depth to ice cement in Altar till varies from 10 to 45 cm.

4.2.3. Sessrumnir till

Sessrumnir till was deposited in the middle Miocene (>14.8 Ma) by wet-based alpine glaciers in the western Dry Valleys region (Marchant et al., 1993b). Sessrumnir

till typically contains 10% gravel, 70% sand, and 20% mud. For the most part, below a surface pavement of large cobbles, it lacks clasts >64 mm in size (Marchant et al., 1993b). The depth to ice cement in this unit varies from 10 cm to >1 m.

5. Numerical models

Modeling efforts were divided into three parts. First, we modeled seasonal changes in thaw depths that would arise from prescribed increases in mean summertime soil surface temperatures (MSSST, see definition in Fig. 5). Second, we modeled the minimum thaw depths required to facilitate failure by shallow planar sliding in each deposit. For this, we assumed that the present soil moisture conditions were maintained, i.e., that during the interval of prescribed warming, years to decades long, soils maintained their current

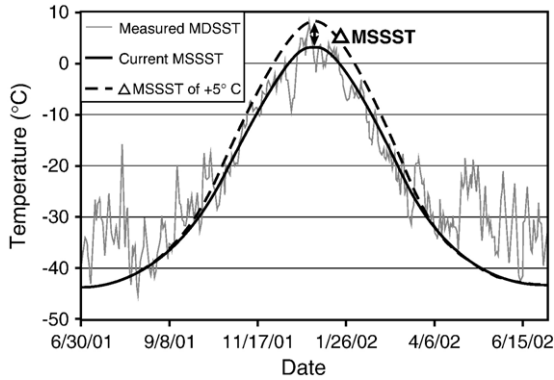


Fig. 5. A one-year record of soil-surface temperature at ~1200 m elevation on the floor of central Beacon Valley [data from Long-term Ecological Research: huey.Colorado.edu/LTER/meteordata.html]. The solid grey line shows measured mean daily soil surface temperature (MDSST); the solid black line, the mean summertime soil surface temperature (MSSST). The dashed line indicates a Δ MSSST of +5 °C.

GWC (as discussed below this is likely an oversimplification, and one that makes our results conservative, see Discussion). Third, we modeled subsurface water flow as a function of sediment texture (Darcy flow); this is required because hydraulic conductivity bears critically on pore pressures and the stability of these ice-cemented deposits.

5.1. Soil temperature calculations

The depth- and time-dependent variations in subsurface soil temperatures that arise from prescribed increases in MSSST were solved using a one-dimensional heat diffusion equation:

$$\frac{\partial T}{\partial t} = \kappa \frac{\partial^2 T}{\partial z^2} \quad (1)$$

where T is temperature, t is time, κ is thermal diffusivity and z is depth. Geothermal heat can be excluded from the model because temperatures in the upper meter of the soil are controlled by atmospheric temperature. Daily fluctuations in ground-surface temperatures do not propagate below ~15-cm depth, whereas seasonal fluctuations propagate to ~5-m depth (Kowalewski et al., 2006). Because the depths of thaw required to initiate slope failures greatly exceed 15-cm depth (see results below), we ignore the shallow, high-frequency temperature extremes observed during daily fluctuations (Figs. 4 and 5). Seasonal variations in thermal diffusivity (e.g. the increase in winter thermal diffusivities of 18% over summer diffusivities observed in Dry Valley soils (Pringle et al., 2006)) were not included as our

thermal model is designed to address changes in mean summertime temperatures only.

The thermal diffusion equation (Eq. (1)) was solved using finite difference methods (central difference formulation). The model domain extended from 0-m to 10-m depth and the model was run for one year (in which the initial time step was set at July 1). The modeled subsurface temperatures were solved at 15-min time intervals and 5-cm space intervals. For all model runs, initial conditions were set as an exponential increase with depth, with -45 °C at the soil surface and -20 °C at 10-m depth (consistent with our measurements in Fig. 4 (Kowalewski et al., 2006) and Long-term Ecological Research: huey.Colorado.edu/LTER/meteordata.html):

$$T(z_i) = T(z_{i-1}) + (1.182 * e^{-0.469z_i}) \quad (2)$$

where T is temperature, z_i is a given node in discretized space, and z_{i-1} is a previous node in space.

The boundary conditions for the base of the model domain were set at a constant temperature of -20 °C. At the soil surface, boundary temperature conditions were modeled as a modified sine curve (to account for abrupt, short duration, and intense Dry Valley summers):

$$T(t) = T_S + \Delta T_0 \cos(\omega[t + \alpha \sin(\omega t)]) \quad (3)$$

where T is temperature, t is time, T_S is the mean soil surface temperature, ΔT_0 is the amplitude of the sine wave, ω is the angular wavelength, and α is a correction factor (units of time; here 30 days) to model abrupt summer temperatures (Fig. 5).

Latent heat of fusion (334 kJ/kg for ice) is an important factor in controlling ground temperatures in permafrost regions (Nixon and McRoberts, 1973). Therefore, we ran two ground temperature models, one with heat transfer via conduction only and another that combined conduction with latent heat of fusion. To account for latent heat, we first calculated the mass of ice contained in a square-meter of soil centered at each depth node in our finite-difference model. Setting the phase change between ice and water at $T(z)=0$, we converted temperature changes over each time-step (calculated using Eq. (1)) into heat energy using the following relationship:

$$Q = mc_t \Delta T \quad (4)$$

where Q is heat energy, m is total mass, c_t is the total specific heat capacity of the soil and ΔT is change in temperature. The energy was used to melt the ice at each node, buffering the node at 0 °C until all of the ice had melted. Specific heat capacity, diffusivity, and conductivity

were calculated by averaging soil properties (sediment, ice, water, air) at each node (Table 2).

5.2. Slope stability calculations

Slope stability is described in terms of a safety factor (F_S), a unitless ratio of shear strength to applied shear stress that can be defined as:

$$F_S = \frac{c' + (\gamma - m\gamma_w)z_p \cos^2 \theta \tan \phi'}{\gamma z_p \sin \theta \cos \theta} \quad (5)$$

where c' =effective cohesion, γ =unit weight of soil, m =ratio of the height of the water table (fully saturated conditions) above the slip plane to the total height of the soil column, γ_w =unit weight of water, z_p =depth to slide plane, θ =slope angle, and ϕ' =effective angle of internal friction (Fig. 6; Table 2) (McRoberts and Morgenstern, 1974).

From Eq. (5), we determined the percentage of saturation (m) required to induce failure as a function of depth to the slide plane (z_p) by setting $F_S=1$ and solving for m .

$$m = \frac{\left(\gamma - \frac{\gamma z_p \sin \theta \cos \theta - c'}{z_p \cos^2 \theta \tan \phi} \right)}{\gamma_w} \quad (6)$$

Thaw depth and slide depth are assumed to be coincident. Our model considers changes in saturation (m) as a function of changes in the depth to the slide plane (z_p). This is different from most slope failure analyses that generally model changes in saturation from external sources (i.e. precipitation) for a constant

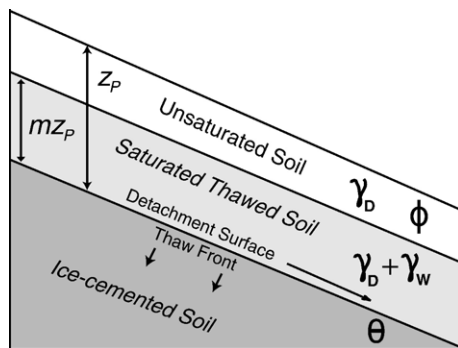


Fig. 6. Schematic showing model parameters within the upper meter of thawing soil, where mz_p =the thickness of saturated soil; z_p =depth to slide plane; γ_w =unit weight of water; γ_d =unit weight of dry soil; γ =total unit weight of soil (which varies with depth and is not shown on the graph); ϕ' =effective angle of internal friction; and θ =slope angle. The thaw front is assumed to be parallel to the ground surface. Given that saturation is derived solely from thawing of interstitial ice, m varies with changes in z_p .

slide depth. However, because the moisture source is internal in our model (solely from the melting of interstitial ice), the degree of saturation varies as a function of thaw depth according to the following equation (which assumes that the thaw front is parallel with the ground surface and that all moisture is retained in the system):

$$m = \frac{W}{p} \left(1 - \frac{z_{IC}}{z} \right) \quad (7)$$

where m is the percentage of the soil that is saturated as a function of depth, W is the volumetric water content, p is the porosity, z_{IC} is the initial depth of the ice-cement table, and z is depth (Table 2).

The GWC in the unsaturated zone was set at 0%. The coarse texture of most soils implies that upward migration of water from the saturated zone to the unsaturated zone by capillary suction would be minimal with subsurface melt. Also, water retention in the unsaturated zone, if present from the melting of surface snowfall, would likewise be minor.

5.3. Subsurface water flow

We estimated the flow rates for subsurface meltwater produced by thawing of ice cement. The key question is whether rapid rates of subsurface water flow would prevent high pore pressures required for planar sliding. For each deposit, we examined downslope water flow using Darcy's Flow Law through porous media:

$$q = k_H \frac{dh}{dl} \quad (8)$$

where q is specific discharge, k_H is hydraulic conductivity, and dh/dl is the hydraulic gradient that varies by the slope angle (θ).

Hydraulic conductivity (k_H) was determined through permeability and conductivity experiments reported in Marchant et al. (2002), and through analyses of the grain size distribution, porosity, and average pore size:

$$k_H = \frac{GeR_c^2\gamma_w}{\mu} \quad (9)$$

where Ge is the geometrical shape of the pores, R_c is average pore size (Eq. (10)), γ_w is the density of water, and μ is the water's viscosity. Average pore sizes were determined using the following equation:

$$R_c = \frac{p}{b} \sum_{i=0}^n x_n d_n \quad (10)$$

where p is the percent of the volume filled by pores, b is the percent of the volume filled by particles, d is the average particle size in a specific size fraction (i.e. silt, fine sand, gravel, etc.), x is the percentage of the soil that is within that specific fraction.

6. Model results

6.1. Dolerite-rich colluvium

The colluvial deposits studied here contain sufficient subsurface moisture (ice) such that planar sliding *should theoretically* occur when thawing reaches a depth of 30–35 cm, but only by assuming 100% water retention and ignoring the very significant flux of meltwater through these coarse-grained deposits (see below). A thaw depth of 30–35 cm corresponds to a change in mean summertime soil surface temperature (Δ MSSST; Fig. 5) of 4 °C (with heat transfer via conduction only) or

6 °C (with conductive heat transfer including the effects of latent heat) (Table 2 and Fig. 4). Although theoretically possible, we contend that dolerite colluvium is, in fact, insensitive to shallow sliding; results from Eq. (8) indicate that flow rates of subsurface meltwater could be as much as ~ 40 m/day, roughly four orders of magnitude greater than the meltwater generated from thawing of ice cement (the vertical thaw rate of ice cement in dolerite colluvium is calculated from Eqs. (1)–(4) at ~ 1.2 – 1.4 cm/day). Hence, although Eqs. (1)–(4) predict failure of dolerite colluvium with a Δ MSSST of ~ 4 to 6 °C, the rapid rate of subsurface water flow is prohibitive. We note, however, that other types of mass wasting and slope erosion (via debris flows, channel incision from meltwater, groundwater seeps associated with subsurface water flow, etc.) could be operative with a temperature increase of 4 to 6 °C (e.g., Marchant and Denton, 1996; Lyons et al., 2005), but these processes lie beyond the scope of this paper.

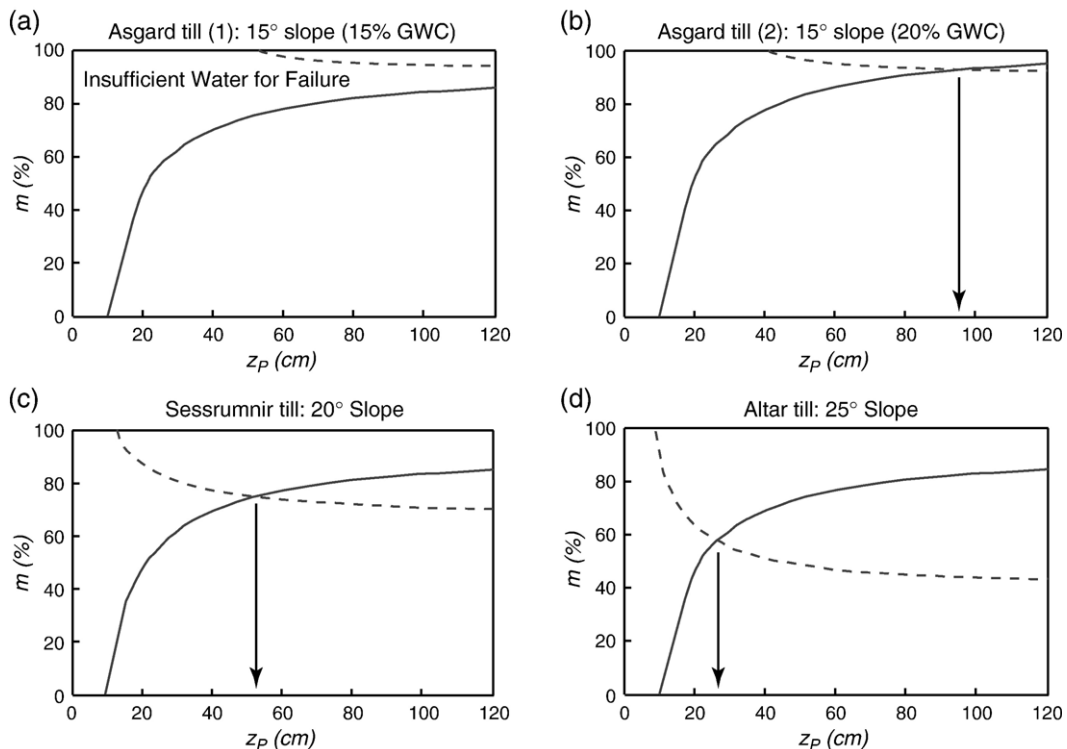


Fig. 7. Results for sensitivity tests of various silt-rich deposits showing thaw depths required for failure (arrowed); m (%) is fully saturated soil and z_p is depth to the slide plane. The dotted lines (in a through d) represent the minimum saturation (as a function of depth) required to induce failure, whereas the solid lines show the level of saturation that would result from depth-dependent thawing of ice cement for each given soil. The intersection of these two lines (and the vertical arrow that marks this intersection) corresponds to the minimum thaw depth at which there is sufficient soil moisture to induce failure. Individual panels: (a) Asgard till on a slope of 15°, and with an ice-cement table at 10-cm depth (15% GWC); this soil configuration is insensitive to failure due to insufficient subsurface GWC. (b) Asgard till on a slope of 15°, but with GWC of 20%; this deposit could fail if thaw-depths are ≥ 95 cm. (c) Sessrumnir till on a slope of 20° and with an ice-cement table at 10-cm depth (15% GWC); this deposit could fail if thaw-depths are ≥ 52 cm. (d) Altar Till on a slope of 25° and with an ice-cement table at 10-cm depth (15% GWC); this deposit could fail if thaw-depths are ≥ 28 cm.

6.2. Asgard till, Sessrumnir till, and Altar till

Results for slope stability analyses of fine-grained deposits (Asgard till, Sessrumnir till, and Altar till) are shown in Fig. 7a through d, all of which plot potential slide depths (z_p) as a function of saturation (m). Calculated rates of Darcy flow are significantly less than for dolerite colluvium, averaging between ~ 30 and 80 cm/day (Table 3); this relatively slow flow enables the build up of requisite pore pressures, at least for soils in which shallow ice cement contains a minimum GWC of $\sim 15\%$.

Asgard till that overlies a gentle slope of 15° and exhibits a shallow ice-cement table at 10-cm depth (GWC of 15%) (Figs. 7a and 8a) would likely remain stable (even with thawing to >1 m depth) due to insufficient moisture availability. Conversely, Asgard till in a similar setting but with 20% GWC at ≥ 10 -cm depth could fail with thawing to ≥ 95 cm (Fig. 7b). If employing a purely conductive heat-transfer model for soils (Eq. (1)), this thaw depth corresponds to a Δ MSSST of 10°C ; when including the effects of latent heat in our models, it requires a Δ MSSST of 14 – 15°C (Fig. 8b). Our model results for Sessrumnir till and Altar till show greater sensitivity to thaw-induced planar sliding. For example, Sessrumnir till on a slope of 20° and with an ice-cement table at 10-cm depth (GWC 15%) (both common in the Dry Valleys region) could fail with thaw to ≥ 52 cm (Fig. 7c). This depth of thaw corresponds to a Δ MSSST of 6°C (conduction model) or 8.5°C (conduction and latent heat model) (Fig. 8c). Likewise, Altar till on a slope of $\sim 25^\circ$ and with an ice-

cement table at 10-cm depth (GWC 15%) would most probably fail by planar sliding with thaw to ≥ 28 cm (Fig. 7d). This thaw depth corresponds to a Δ MSSST of 3.5°C (conduction model) or 5°C (conduction and latent heat model) (Fig. 8d).

Because the mean summertime soil surface temperatures (MSSST) in the stable upland zone appear to track linearly the changes in summertime atmospheric temperatures (Kowalewski et al., 2006), and because we can model subsurface changes in soil temperature using Eqs. (1)–(4), our modeling results suggest that ice-cemented, silt-rich deposits of the stable upland zone (on slopes $\geq 20^\circ$) could experience planar-sliding if summertime atmospheric temperatures increase ~ 4 to 9°C above present values (see Fig. 8a–d, and caption).

7. Discussion

The results of our six sensitivity tests highlight the importance of soil texture, GWC, slope angle, and depth to the ice-cement table on slope stability. In general, the most sensitive deposits are silt-rich, occur on steep slopes, and contain ice cement with $\geq 15\%$ GWC at <20 -cm depth.

7.1. Boundary conditions and modern analogs from coastal sites in the McMurdo Dry Valleys

As noted above, all variables in our modeled scenarios other than ground-surface temperature (i.e., MSSST) remain constant and match current, measured

Table 3
Synthesis of the model results for the six sensitivity tests

Deposit	Parameters	Sediment texture (<16 mm fraction)	Thaw depth (cm)	Δ MSSST (conduction) ($^\circ\text{C}$)	Δ MSSST (conduction and latent heat) ($^\circ\text{C}$)	Average Darcy flow rate (cm/day)	Failure?
Colluvium (1)	32° slope 12% GWC	1% mud 39% sand 60% gravel	≥ 30	4	6	4000–6000	No
Colluvium (2)	26° slope 20% GWC	2% mud 57% sand 41% gravel	≥ 35	4	6	2000–4000	No
Asgard till (1)	15° slope 15% GWC	18% mud 56% sand 26% gravel	Insufficient water	N/A	N/A	30–50	No
Asgard till (2)	15° slope 20% GWC	18% mud 56% sand 26% gravel	≥ 95	10	14.5	30–50	Yes
Sessrumnir till	20° slope 15% GWC	20% mud 70% sand 10% gravel	≥ 52	6	8.5	40–60	Yes
Altar drift	25° slope 15% GWC	13% mud 60% sand 27% gravel	≥ 28	3.5	5	50–80	Yes

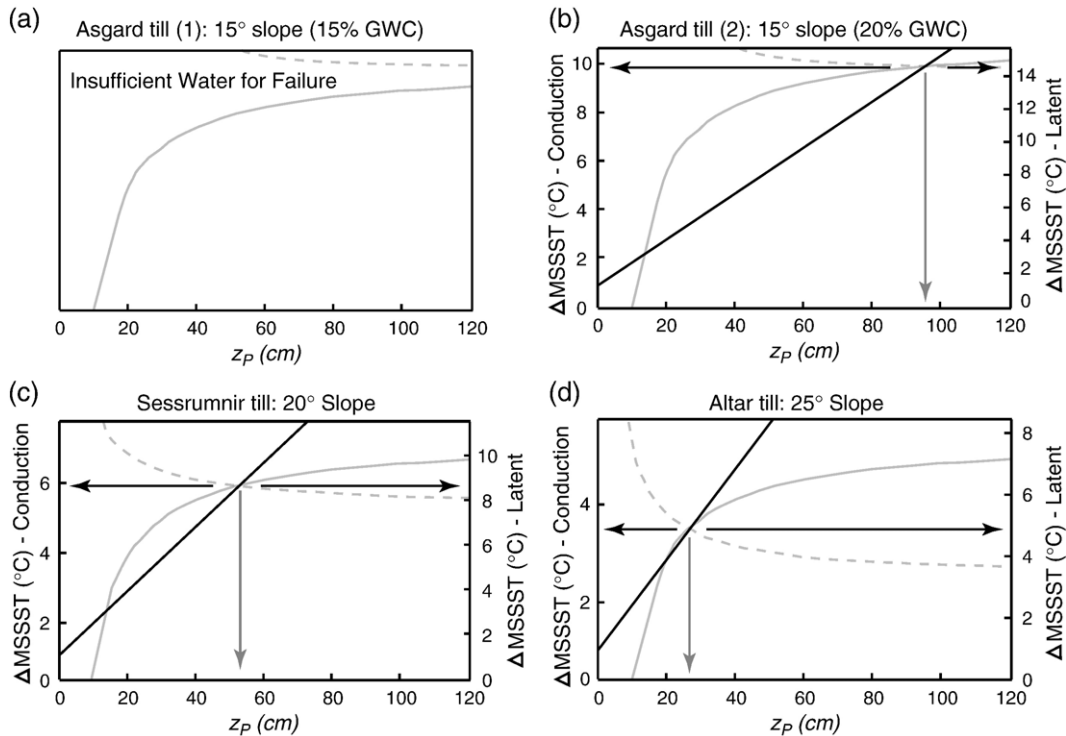


Fig. 8. Results for the thaw depths that would occur with prescribed changes in mean summertime soil surface temperatures (ΔMSSST ; see Fig. 5). The left y-axis denotes thaw depths using a purely conductive thermal model, whereas the right y-axis is based on our model that includes heat transfer via conduction and latent heat of fusion. Note that when the effects of latent heat are included in our model, the thaw rate slows by $\sim 35\%$. Panels a–d show conditions for failure (if possible) for our test scenarios; boundary conditions for each deposit are identical to those described in Fig. 7. Panel b shows that failure of Asgard till would require a ΔMSSST of 10 °C (conduction-only model) or 14.5 °C (conduction with latent heat included). Higher angle slopes modeled for Sessrumnir till (c) could fail with a ΔMSSST of 6 °C (conduction-only model) or 8.5 °C (conduction with latent heat included); for Altar till (d) slopes could fail with a ΔMSSST of 3.5 °C (conduction-only model) and 5 °C (conduction with latent heat included).

conditions. Given that a change of 4 to 9 °C in MSSST would likely evolve over decades, if not centuries, it is unlikely that soil-moisture conditions prior to thawing would be exactly the same as they are today. However, as described below we expect that an increase in MSSST of 4 to 9 °C would be accompanied by an overall increase in soil moisture, both in terms of an increase in the GWC of ice cement and a shallowing of the ice-cement table. These are trends that would tend to increase the sensitivity of most slopes to thaw-induced planar sliding.

The soil-moisture conditions within the relatively warm coastal thaw zone (Table 1) provide a good analog for upland soils in a warmer climate. Soils in the coastal thaw zone often exhibit shallow ice tables (~ 10 cm) with $\text{GWC} \gg 20\%$ (Campbell et al., 1997a; Campbell and Claridge, 2006). They also show abundant evidence for thermokarst, solifluction, and slides (Marchant and Denton, 1996; Marchant and Head, in press; Denton and Marchant, 2000). Meltwater in this zone is generated from melting snowbanks and glaciers. Snowbanks, in

turn, are replenished by relatively significant snowfall in this warm zone. In general, the geologic evidence from the MDV and adjacent regions suggests that as atmospheric temperatures increase, soils become wetter, rather than drier (see also (Denton et al., 1989)). For example, ice-core records from Taylor Dome (a peripheral dome of the East Antarctic Ice Sheet located ~ 35 km west of the MDV) show that during the Holocene warming that followed the last glacial maximum (~ 8 to 10 °C of atmospheric warming) rates of ice accumulation (i.e., precipitation) increased sixfold (Steig et al., 2000). Therefore, we conclude that our model results are conservative in that we maintain artificially dry soil-moisture conditions during periods of prescribed atmospheric warming.

7.2. Broader implications

Greenhouse-induced atmospheric warming over Antarctica could reach as much as 2 to 6 °C during

the next century (Intergovernmental Panel on Climate Change (IPCC), 2001; Torn and Harte, 2006). Hence, if global warming occurs as predicted, and if the stable upland zone experiences an increase in mean summertime soil surface temperatures of ~ 4 to 9 °C, then some ice-cemented, silt-rich deposits that have been stable for millions of years could be at risk from thaw-induced planar sliding.

If we assume that soils in the stable upland zone have not been drier in the past than they are now, then our results could be used to shed light on the maximum possible summertime warming achieved since the drifts were deposited. Assuming that the physical evidence for shallow planar slides would be retained in the geomorphic record, and given that we see no evidence for discrete downslope movement in any of these deposits (Marchant and Denton, 1996) (Fig. 2), we tentatively conclude that mean summertime soil surface temperatures in this region did not rise more than ~ 4 to 9 °C above present values since mid-to-late Miocene time (the age of the silt-rich deposits studied). This assertion is consistent with the preservation of pristine, Miocene-aged ashfall at the ground surface in the upland zone and with the long-term stability of East Antarctic Ice Sheet inland of the MDV (e.g., Sugden et al., 1995).

8. Conclusions

We employed a Mohr–Coulomb-based equation of safety factor to assess the response of ice-cemented slopes in the stable upland zone of the MDV to increases in mean summertime soil surface temperatures (MSSST). Our results show that although most colluvial deposits appear to contain sufficient near-surface ice for thaw instability (ice-table at ~ 10 – 20 cm depth and GWC of $\sim 20\%$), the coarse texture of these deposits enables rapid moisture loss upon thawing, preventing failure by planar sliding. Ice-rich, silty deposits, on the other hand, are sensitive to thaw-induced sliding. Results show that silty deposits on slopes $\geq 20^\circ$ and with shallow ice tables (< 20 cm depth) containing $\sim 15\%$ GWC, all of which are common conditions in the western MDV region, could fail by sliding with an increase in MSSST of ~ 4 to 9 °C. This corresponds to an atmospheric increase of ~ 4 to 9 °C, and lies within the broad envelope of future warming over the next century expected to occur due to greenhouse-gas emissions. If we assume that the current soil-moisture conditions can be applied to slope deposits in the distant past (i.e., millions of years ago), then our results suggest that MSSST, and by inference atmospheric tempera-

tures, in the stable upland zone did not increase by more than ~ 4 to 9 °C above present values since at least late Miocene time.

Acknowledgements

We thank Douglas Kowalewski for excellent assistance in the field and for stimulating discussion during the preparation of the manuscript. Paul Hall provided valuable insight concerning heat transfer and finite difference methods. We also thank Antoni Lewkowicz and Thomas Sheahan for comments during the early stages of this research, as well as three anonymous reviewers whose comments helped to improve this manuscript. Funding for this research was provided by NSF Polar Programs OPP-338291 to DRM.

References

- Ackert, R.P. Jr., 1990. Surficial geology and geomorphology of Njord Valley and adjacent areas of the western Asgard Range, unpublished masters thesis.
- Brook, E.J., Kurz, M.D., Ackert Jr., R.P., Denton, G.H., Brown, E.T., Raisbeck, G.M., Yiou, F., 1993. Chronology of Taylor Glacier advance in Arena Valley, Antarctica, using in situ cosmogenic ^3He and ^{10}Be . *Quat. Res.* 39, 11–23.
- Campbell, I.B., Claridge, G.G.C., 2006. Permafrost properties, patterns and processes in the Transantarctic Mountains region. *Permafr. Periglac. Process.* 17, 215–232.
- Campbell, I.B., Claridge, G.G.C., Balks, M.R., Campbell, D.I., 1997a. Moisture content in soils of the McMurdo Sound and Dry Valley region of Antarctica. In: Lyons, W.B., Howard-Williams, C., Hawes, I. (Eds.), *Ecosystem Processes in Antarctic Ice-free Landscapes*. Balkema, Rotterdam, New Zealand, pp. 61–76.
- Campbell, D.I., MacCulloch, R.J.L., Campbell, I.B., 1997b. Thermal regimes of some soils in the McMurdo Sound region, Antarctica. In: Lyons, W.B., Howard-Williams, C., Hawes, I. (Eds.), *Ecosystem Processes in Antarctic Ice-free Landscapes*. Balkema, Rotterdam, New Zealand, pp. 45–55.
- Davies, M.C.R., Hanza, O., Harris, C., 2001. The effect of rise in mean annual temperature on the stability of rock slopes containing ice-filled discontinuities. *Permafr. Periglac. Process.* 12, 137–144.
- Denton, G.H., Marchant, D.R., 2000. The geologic basis for a reconstruction of a grounded ice sheet in McMurdo Sound, Antarctica, at the last glacial maximum. *Geogr. Ann.* 82A, 167–211.
- Denton, G.H., Bockheim, J.G., Wilson, S.C., Stuiver, M., 1989. Late Wisconsin and early Holocene glacial history, inner Ross Embayment, Antarctica. *Quat. Res.* 31, 151–182.
- Doran, P.T., Prisco, J.C., Lyons, W.B., Walsh, J.E., Fountain, A.G., McKnight, D.M., Moorhead, D.L., Virginia, R.A., Wall, D.H., Clow, G.D., Fritsen, C.H., McKay, C.P., Parsons, A.N., 2002a. Antarctic climate cooling and terrestrial ecosystem response. *Nature* 415, 517–520.
- Doran, P.T., McKay, C.P., Clow, G.D., Dana, G.L., Fountain, A.G., Nylén, T., Lyons, W.B., 2002b. Valley floor climate observations from the McMurdo Dry Valleys, Antarctica, 1986–2000. *J. Geophys. Res.* 107, D244772. doi:10.1029/2001JD002045.

- Harris, C., Davies, M.C.R., Etzelmuller, B., 2001. The assessment of potential geotechnical hazards associated with mountain permafrost in the warming global climate. *Permafrost. Periglac. Process.* 12, 145–156.
- Hindmarsh, R.C.A., van der Wateren, F.M., Verbers, A.L.L.M., 1998. Sublimation of ice through sediment in Beacon Valley, Antarctica. *Geogr. Ann.* 80A, 209–219.
- Intergovernmental Panel on Climate Change (IPCC), 2001. In: Houghton, J.T., et al. (Eds.), *Climate Change 2001: the scientific basis: contribution of Working Group I to the Third Assessment Report of the Intergovernmental Panel on Climate Change*. Cambridge Univ. Press, New York, p. 881.
- Ivy-Ochs, S., Schlüchter, C., Kubik, P.W., Dittrich-Hannen, B., Beer, J., 1995. Minimum ^{10}Be exposure ages of early Pliocene for the Table Mountain plateau and the Sirius Group at Mount Fleming, Dry Valleys, Antarctica. *Geology* 23, 1007–1010.
- Kowalewski, D.E., Marchant, D.R., Levy, J.S., Head III, J.W., 2006. Quantifying summertime sublimation rates for buried glacier ice in Beacon Valleys, Antarctica. *Antarct. Sci.* 18, 421–428.
- Lyons, W.B., Welch, K.A., Carey, A.E., Doran, P.T., Wall, D.H., Virginia, R.A., Fountain, A.G., Csathó, B.M., Tremper, C.M., 2005. Groundwater seeps in Taylor Valley, Antarctica: an example of a subsurface melt event. *Ann. Glaciol.* 40, 200–206.
- Marchant, D.R., Denton, G.H., 1996. Miocene and Pliocene paleoclimate of the Dry Valleys region, southern Victoria Land: a geomorphological approach. *Mar. Microplaeontol.* 27, 253–271.
- Marchant, D.R., Head III, J.W., in press. Antarctic Dry Valleys: morphoclimate zonation, variable geomorphic processes and implications for assessing climate change on Mars. *Icarus*.
- Marchant, D.R., Denton, G.H., Swisher III, C.C., 1993a. Miocene–Pliocene–Pleistocene glacial history of Arena Valley, Quartermain Mountains, Antarctica. *Geogr. Ann.* 75A, 269–302.
- Marchant, D.R., Denton, G.H., Sugden, D.E., Swisher III, C.C., 1993b. Miocene glacial stratigraphy and landscape evolution of the western Asgard Range, Antarctica. *Geogr. Ann.* 75A, 303–330.
- Marchant, D.R., Denton, G.H., Bockheim, J.G., Wilson, S.C., Kerr, A.R., 1994. Quaternary changes in level of the upper Taylor Glacier, Antarctica: implications for paleoclimate and East Antarctic Ice Sheet dynamics. *Boreas* 23, 29–43.
- Marchant, D.R., Denton, G.H., Swisher III, C.C., Potter Jr., N., 1996. Late Cenozoic Antarctic paleoclimate reconstruction from volcanic ashes in the Dry Valleys region of southern Victoria Land. *Geol. Soc. Amer. Bull.* 108, 181–194.
- Marchant, D.R., Lewis, A.R., Phillips, W.M., Moore, E.J., Souchez, R.A., Denton, G.H., Sugden, D.E., Potter Jr., N., Landis, G.P., 2002. Formations of patterned ground and sublimation till over Miocene glacier ice in Beacon Valley, southern Victoria Land, Antarctica. *Geol. Soc. Amer. Bull.* 114, 718–730.
- Margerison, H.R., Phillips, W.M., Stuart, F.M., Sugden, D.E., 2005. Cosmogenic ^3He concentrations in ancient flood deposits from the Coombs Hills, northern Dry Valleys, East Antarctica: interpreting exposure ages and erosion rates. *Earth Planet. Sci. Lett.* 230, 163–175.
- McKay, C.P., Mellon, M.T., Friedmann, E.I., 1998. Soil temperatures and stability of ice-cemented ground in the McMurdo Dry Valleys, Antarctica. *Antarct. Sci.* 10, 31–38.
- McRoberts, E.C., Morgenstern, N.R., 1974. The stability of thawing slopes. *Can. Geotech. J.* 11, 447–469.
- Nixon, J.F., McRoberts, E.C., 1973. A study of some factors affecting the thawing of frozen soils. *Can. Geotech. J.* 10, 439–452.
- Pringle, D.J., Dickinson, W.W., Trodahl, H.J., Pyne, A.R., 2006. Depth and seasonal variations in the thermal properties of Antarctic Dry Valley permafrost from temperature time series analysis. *J. Geophys. Res.* 108, B102474. doi:10.1029/2002JB002364.
- Scambos, T., Hulbe, C., Fahnestock, M., 2003. Climate-induced ice shelf disintegration in the Antarctic Peninsula. *Antarct. Res. Ser.* 79, 79–92.
- Schaefer, J.M., Ivy-Ochs, S., Wieler, R., Leya, I., Baur, H., Denton, G.H., Schluchter, C., 1999. Cosmogenic noble gas studies in the oldest landscape on earth: surface exposure ages of the Dry Valleys, Antarctica. *Earth Planet. Sci. Lett.* 167, 215–226.
- Schaefer, J.M., Baur, H., Denton, G.H., Ivy-Ochs, S., Marchant, D.R., Schluchter, C., Wieler, R., 2000. The oldest ice on Earth in Beacon Valley, Antarctica: new evidence from surface exposure dating. *Earth Planet. Sci. Lett.* 179, 91–99.
- Schellart, W.P., 2000. Shear results for cohesion and friction coefficients for different granular materials: scaling implications for their usage in analogue modeling. *Tectonophysics* 324, 1–16.
- Steig, E.J., Morse, D.L., Waddington, E.D., Stuiver, M., Grootes, P.M., Mayewski, P.A., Twickler, M.S., Whitlow, S.I., 2000. Wisconsinan and Holocene climate history from an ice core at Taylor Dome, Western Ross Embayment, Antarctica. *Geogr. Ann.* 82A, 213–235.
- Stuiver, M., Yang, I.C., Denton, G.H., Kellogg, T.B., 1981. Oxygen isotope ratios of Antarctic permafrost and glacier ice. In: McGinnis, L.D. (Ed.), *Antarctic Research Series: Dry Valley Drilling Project*, vol. 33. American Geophysical Union, Washington, D.C., pp. 131–139.
- Sugden, D.E., Denton, G.H., Marchant, D.R., 1995. Landscape evolution of the Dry Valleys, Transantarctic Mountains: tectonic implications. *J. Geophys. Res.* 100, 9949–9967.
- Summerfield, M.A., Stuart, F.M., Cockburn, H.A.P., Sugden, D.E., Dunai, T., Marchant, D.R., 1999. Long-term rates of denudation in the Dry Valleys, Transantarctic Mountains, southern Victoria Land, Antarctica based on in-situ-produced cosmogenic ^{21}Ne . *Geomorphology* 27, 113–129.
- Torn, M.S., Harte, J., 2006. Missing feedbacks, asymmetric uncertainties, and the underestimation of future warming. *Geophys. Res. Lett.* 33, L10703. doi:10.1029/2005GL025540.